



HAL
open science

Mesenchymal stem cell interacted with PLCL braided scaffold coated with poly- l -lysine/hyaluronic acid for ligament tissue engineering

Xing Liu, Cédric Laurent, Qiaoyue Du, Laurie Targa, Ghislaine Cauchois, Yun Chen, Xiong Wang, Natalia de Isla

► To cite this version:

Xing Liu, Cédric Laurent, Qiaoyue Du, Laurie Targa, Ghislaine Cauchois, et al.. Mesenchymal stem cell interacted with PLCL braided scaffold coated with poly- l -lysine/hyaluronic acid for ligament tissue engineering. *Journal of Biomedical Materials Research Part A*, 2018, 106 (12), pp.3042-3052. 10.1002/jbm.a.36494 . hal-02070806

HAL Id: hal-02070806

<https://hal.science/hal-02070806v1>

Submitted on 4 Apr 2022

HAL is a multi-disciplinary open access archive for the deposit and dissemination of scientific research documents, whether they are published or not. The documents may come from teaching and research institutions in France or abroad, or from public or private research centers.

L'archive ouverte pluridisciplinaire **HAL**, est destinée au dépôt et à la diffusion de documents scientifiques de niveau recherche, publiés ou non, émanant des établissements d'enseignement et de recherche français ou étrangers, des laboratoires publics ou privés.

1 **Mesenchymal stem cell interacted with PLCL braided scaffold coated with**
2 **Poly-L-lysine/Hyaluronic Acid for Ligament tissue engineering**

3 Xing Liu¹, Cédric Laurent², Qiaoyue Du³, Laurie Targa¹, Ghislaine Cauchois¹, Yun Chen³, Xiong
4 Wang¹, Natalia de Isla¹

5 ¹*CNRS UMR 7365 - Université de Lorraine, Ingénierie Moléculaire et Physiopathologie Articulaire (IMoPA),*
6 *Vandœuvre-lès-Nancy, France*

7 ²*CNRS UMR 7239 LEM3 - Université de Lorraine, Vandœuvre-lès-Nancy, France*

8 ³*Department of Biomedical Engineering, School of Basic Medical Science, Wuhan University, Wuhan, China*

9 Correspondence to: xing.liu@univ-lorraine.fr; natalia.de-isla@univ-lorraine.fr

10 **Abstract:** The challenge of finding an adapted scaffold for ligament tissue
11 engineering still remains unsolved after years of researches. A technology to fabricate
12 a multilayer braided scaffold with flexible and elastic Poly (L-lactide-co-caprolactone)
13 (PLCL 85/15) has been recently pioneered by our team. In the present study,
14 polyelectrolyte multilayer films (PEM) with poly-L-lysine (PLL)/ hyaluronic acid
15 (HA) were deposited on this scaffold. After PEM modification, polygonal (PLL) and
16 particle-like (HA) structures were present on the braided scaffold with no significant
17 variation of fibers Young's modulus. Wharton's Jelly Mesenchymal Stem Cells
18 (WJ-MSC) and Bone Marrow Mesenchymal Stem Cells (BM-MSC) showed good
19 metabolic activity on scaffolds. They presented a spindled shape along the fiber
20 longitudinal direction, and crossed the fibers to form cell bridges. Collagen type I,
21 collagen type III and tenascin-C secreted by MSCs were detected on day 14.
22 Moreover, one-layer modified scaffold presented increased chemotaxis. As a
23 conclusion, our results indicate that this braided PLCL scaffold with one layer PEM
24 modification shows inspiring potential with satisfying mechanical properties and

1 biocompatibility. It opens new perspectives to incorporate growth factors within
2 PEM-modified braided PLCL scaffold for ligament tissue engineering and to recruit
3 endogenous cells after implantation.

4 **Keyword:** Poly (L-lactide-co-caprolactone), braided scaffold, mesenchymal stem cell,
5 polyelectrolyte multilayer films, ligament tissue engineering

6 **Introduction**

7 Ligament injuries are among the highest incidence of musculoskeletal disorders,¹⁻⁴
8 especially for the people who commonly do sports, rigorous physical activities, suffer
9 acute trauma, or for aged people. The main strategy for repairing injured ligament
10 consists in a surgical intervention called ligamentoplasty. Grafts⁵⁻⁷ used in such
11 interventions include autografts, allografts, and artificial substitutes. These therapies
12 are subject to constant improvements,^{5,8} resulting in the increase of joint stability,
13 recovered mechanical properties, and patients' overall satisfaction. However, such
14 surgeries are still associated with drawbacks^{9,10} including donor site morbidity,
15 immune rejection, or limited graft sources. With the rise of tissue engineering,
16 ligament tissue engineering could constitute a novel, attractive and alternative
17 approach to recover the function of injured ligament.^{1, 3, 7}

18 Scaffolds with the architectures of sponges, knitted fibers, meshes, hydrogels, wired
19 yarns, and braided fibers have already been reported^{3, 11, 12} in ligament tissue
20 engineering. Despite their benefits, they also suffer from some drawbacks,^{3, 12, 13} such

1 as insufficient mechanical properties, brittle behavior, or lack of functional groups for
2 molecular signaling. In our previous studies,^{14, 15} PLCL has been used to develop a
3 novel multilayer braided scaffold. It presents a porous structure for cell or tissue
4 ingrowth, nutrient exchange, and post-graft degradation. Thanks to the adjustable
5 geometrical parameters of this architecture (e.g. number of layers, fiber diameter and
6 braiding angle), the mechanical strength could also be adjusted to fulfill requirements
7 of different ligaments. PLCL is a synthetic biodegradable co-polymer with high
8 elasticity consisting of polylactide (PLLA) and polycaprolactone (PCL). It has already
9 been pointed out¹⁶ to support tendon cell proliferation, and has been widely applied in
10 tissue engineering because of its good biocompatibility and mechanical properties.

11 Seeding cells¹⁷⁻¹⁹ could also contribute to the functionality of tissue engineered
12 constructs by encouraging its colonization and extra cellular matrix (ECM) synthesis.
13 Ligament fibroblasts¹⁹ may appear as natural candidate reparative cells for ligament
14 tissue engineering, but there are limited by cell availability, quantity of donors and
15 also differentiation capacity. Because of self-renew ability, differentiation potential,
16 and bioactive molecule secretion activity, Mesenchymal Stem Cells (MSCs) have
17 become a popular cell source applied in tissue engineering.^{17, 20} In addition, MSCs
18 have already been reported^{17, 20} to proliferate better and produce more collagen than
19 fibroblasts. Wharton's Jelly Mesenchymal Stem Cells (WJ-MSC) and Bone Marrow
20 Mesenchymal Stem Cells (BM-MSC) were thus selected as cell sources in our present
21 study.

1 In the last decades, Layer-By-Layer (LBL) technology has been widely used to
2 modify the surface of biomaterials in order to improve the integration or add
3 specialized properties to scaffolds.^{21, 22} Examples of LBL biological applications
4 include mediation of cellular functions to promote cell adhesion, proliferation,
5 differentiation; biosensors; drugs or bioactive molecular delivery system, and
6 biomimetics. The cellular adhesion and homogeneous cell distribution on the scaffold
7 is a primary element in tissue engineering, and many studies^{7, 23} have emphasized the
8 importance of growth factors to promote MSCs attachment, proliferation, and matrix
9 synthesis in the process of ligament/tendon repair. In the light of the advantages of
10 LBL technology for cell adhesion, and the demand of growth factor delivery system
11 for tissue engineering, LBL modification was introduced in our study in order to
12 promote a ligamentous tissue. Poly-L-lysine (PLL) and Hyaluronic Acid (HA) were
13 selected^{24, 25} as polycation and polyanion for PEM. HA, as a component of
14 extracellular matrix, plays an important role in improving cell growth, differentiation
15 and migration, but it has been observed to be non-adhesive to cells.^{24, 26} On the
16 contrary, PLL has been shown^{27, 28} to promote cell adhesion and it has widely been
17 used for biomaterial coating and drug delivery. The pair of PLL/HA PEM was
18 expected to be an effective system to improve MSCs behavior on scaffolds.

19 Prior to any incorporation of growth factors into a LBL-treated scaffold, it is crucial
20 to study the effect of PLL/HA LBL modification on the behaviors of WJ-MSC and
21 BM-MSC on PLCL braided scaffold. Therefore, in the present contribution the effect

1 of LBL technology on MSCs proliferation, distribution, morphology, collagen
2 synthesis, tenascin-C expression and migration were evaluated, as well the
3 consequence of this treatment on scaffold topology, and mechanical properties.

4 **METHODS AND MATERIALS**

5 **Scaffold fabrication**

6 PLCL (85/15) braided scaffold was fabricated according to previously described
7 methods.^{14, 15} Briefly, it consists of a multilayer braided structure, each layer being
8 made up of 16 fibers of poly(lactide-co- ϵ -caprolactone) (PLCL, Purac Biomaterials)
9 with a lactic acid/ ϵ -caprolactone proportion of 85/15. The polymer was firstly
10 processed into 170 μ m fibers using a homemade extrusion machine at 180°C. Fibers
11 were collected on bobbins, and 16 bobbins were installed on a maypole braiding
12 machine (Composite & Wire Machinery, United States) to form braided scaffolds. Six
13 layers were superposed in total, for a resulting scaffold of 96 fibers measuring around
14 4mm in diameter.

15 **Scaffold modification with LBL technology**

16 PLL (Sigma) and HA (Acros) were dissolved in the NaCl-Tris buffer (pH6.3) at a
17 concentration of 1 mg/mL respectively. Scaffolds were cut into 1 cm-long parts. Firstly,
18 scaffolds were immersed into PLL solutions for 7 min, then gently rinsed in NaCl-Tris
19 buffer for 1 min. They were subsequently introduced into HA solution for 7 min, and
20 then rinsed. Scaffold-blank (SB) refers to the scaffold without LBL modification;
21 scaffold-PLL (SP) refers to scaffold modified only by PLL solution, and
22 scaffold-PLL-HA-PLL (S1L) refers to one-layer modification. This configuration

1 (pH6.3 and only one-layer modification) was selected based on preliminary studies
2 briefly reported in supplementary material.

3 **Scaffold characterization**

4 **Characterization of scaffold by Fourier Transform Infrared Spectroscopy (FTIR)**

5 PLCL fibers were vacuum-dried at 60°C for 24 h, and cut into fine powders for the
6 measurements by FTIR. The dry powders were mixed with Potassium bromide (KBr),
7 and spectra were recorded on an FTIR spectrometer (Nicolet, USA) over the
8 wavenumber range from 4000 to 600 cm⁻¹.

9 **Detecting of PLL/HA coating by Atomic Force Microscopy (AFM) and Confocal**

10 **Laser Scanning Microscopy (CLSM)**

11 The surface of modified fibers was characterized by AFM (Oxford instruments). PLCL
12 fibers were cut into 1 cm and maintained on a glass slide. Surface topology was
13 observed and recorded in contact mode.

14 PLL-FITC (Sigma) was used to replace PLL in PLL/HA system. Fibers were
15 immersed in PLL-FITC/HA solution using the procedure described above, then
16 detected by CLSM (Nikon).

17 **Scaffold morphology by Scanning Electronic Microscopy (SEM)**

18 Scaffolds were frozen with liquid nitrogen for 10 min, dried with vacuum oven for 7 h,
19 then coated with gold and observed by SEM (TESCAN, Czech).

20 **Mechanical properties of fibers**

21 The mechanical properties of PLCL fibers were assessed using tensile tests performed

1 with a Zwick Roell 2.5 device (Zwick, Germany), at a tensile speed of $0.1\text{mm}\cdot\text{s}^{-1}$. Six
2 10 cm-long fibers were tested in parallel for SB, SP and S1L (n=4). The following
3 loading cycle was prescribed 1) 1% strain then unloading 2) 3% strain then unloading 3)
4 increasing strain up to failure. Young's modulus was measured for each sample from
5 the slope of the stress-strain curve just after the first unloading cycle (at 1% of strain).

6 **Mesenchymal Stem Cell isolation and expansion**

7 Human bone marrow and human umbilical cords were supplied by CHRU Hospital and
8 Maternity Hospital (Nancy, France) with the informed consent of donors. Firstly, 25 mL
9 α -MEM (Lonza) medium containing 10% fetal calf serum (FCS, Dominique Dutscher),
10 2 mM L-glutamine (Sigma), 100 U/mL penicillin /streptomycin (Gibco) and 1 $\mu\text{g}/\text{mL}$
11 amphoterin B (Gibco) was added to 20 mL bone marrow, and centrifuged 300g for 5
12 min. The supernatant was removed, and cells were seeded on tissue culture plates at the
13 density of 5×10^4 cells/cm², and then incubated in 37°C, 5% CO₂, 90% humidity until
14 the cells reach 70% - 80% confluence.

15 Human umbilical cord was washed with 70% ethanol and cut into 3-4 cm long samples
16 in the HBSS buffer. The cord was opened to peel off two arteries and one vein; the jelly
17 was torn off from cordon and cut into fine pieces in HBSS buffer. After 7 days, jelly
18 was removed, and the culture medium was changed twice a week until the cells reach
19 70% - 80% confluence. All MSCs used for assays were in passage 3 (P3). Before
20 seeding cells on scaffolds, the quality of MSCs was controlled by testing biological
21 properties as CFU test, senescence test and phenotype characterization. (data shown in

1 supplementary material)

2 **MSC culture on scaffold**

3 Firstly, scaffolds were immersed in ethanol for 30 min, then sterilized with UV for 30
4 min. MSCs were distributed on scaffold (3×10^5 cells, 50 μL /scaffold).
5 MSC-scaffolds were kept in incubator for 30 min, then supplied with 0.95 mL α -MEM
6 complete medium including 100 $\mu\text{g}/\text{mL}$ ascorbic acid (Sigma) and cultured for two
7 weeks.

8 **Evaluation of cell biocompatibility on the scaffolds**

9 **Cell metabolic activity of MSCs on scaffold**

10 Alamar Blue (AB) tests were performed on day 1, 3, 5, and 7. 1 mL 10% AB work
11 solution (Thermo Fish scientific) was added to each scaffold, and incubated for 4 h.
12 The absorbance was measured at 570 nm and 600 nm (n=3). Negative control was AB
13 working. The percentage of Alamar Blue Reagent reduction was calculated according
14 to manufacturer's instructions.

15 **Cell morphology and distribution on scaffold**

16 **Scanning Electronic Microscopy (SEM)**

17 MSC-Scaffolds were firstly fixed with 2.5% glutaraldehyde at 4°C overnight on day 14,
18 then washed with PBS three times. MSC-scaffolds were frozen with liquid nitrogen for
19 10 min, dried with vacuum oven for 7 h, and then images were taken by SEM.

20 **Confocal microscopy**

21 Firstly, MSC-scaffolds were fixed with 1% paraformaldehyde for 10 min at room

1 temperature, then washed with PBS three times. Permibilization treatment was
2 performed by adding 1 mL 0.5% triton-PBS to each well for 20 min and washed with
3 PBS three times. 250 μ L Alexa 488 Phalloidin (Life technologies) solution was
4 supplied to each MSC-scaffold for 45 min, then washed with PBS three times. 200 μ L
5 DAPI (1/2000) (Sigma) was added to each scaffold for 15 min, and washed with PBS
6 three times. Images were taken by confocal microscopy (Leica SP5-CFS).
7 Quantification of cell nuclear elongation was performed by Image J software version
8 1.51k. The length was defined as the longest distance through nucleus and the width
9 was defined as the distance perpendicular to the length. Cell nuclear aspect ratio was
10 calculated by dividing the length to the width. The area of cell nucleus ($n \geq 100$ from
11 more than three images) was measured by Image J 1.51k.

12 **Extracellular matrix synthesized by MSCs on scaffold**

13 After 2 weeks, MSC-scaffolds were firstly fixed with 1% paraformaldehyde for 10 min,
14 then washed with PBS three times. 5% PBS-BSA blocking buffer was added to
15 scaffolds for 30 min. The first antibody anti-collagen type I (CALBIOCHEM),
16 collagen type III (Sigma) and anti-tenascin-C (Abcam) were added (250 μ L) to
17 scaffolds for 1 h, then washed with PBS three times. The second antibody anti-Rabbit
18 IgG-Alexa488 (1/50) (Life technologies) and anti-mouse IgG-Alexa488 were
19 distributed (250 μ L) to scaffold for 45 min, then washed with PBS three times. 200 μ L
20 DAPI (1/2000) was added to each scaffold for 15 min. MSC-Scaffolds were washed
21 with PBS three times, and observed by fluorescence microscopy. Negative controls

1 were performed as MSC with only second antibody, and positive controls were tested
2 as fibroblast with anti-collagen I , collagen III and tenascin-c and second antibody
3 (data shown in supplementary material).

4 **Cell Chemotactic assay**

5 PLCL films were fabricated by hot-processing method, and modified with PLL/HA
6 PEM as PLCL braided scaffold treatment. Boyden chamber assay was performed for
7 migration test by using a transwell (Corning® FluoroBlok™) with 0.8 μm pore
8 fluorescence blocking PET track-etched membrane insert according to manufacturer's
9 instructions. The downside of insert was coated with 100 μL collagen for 30 min.
10 MSCs were starved 24 h before cell migration assay. SB, SP, and S1L film with 500
11 μL α-MEM complete medium were introduced to each reservoir. 1.5×10^5 cell
12 suspension in α-MEM without FCS (200 μL) was added into each insert. After 24 h,
13 cells were stained with calcein AM (Thermo Fish scientific) (1/1000) for 30 min, then
14 washed with PBS three times. Cell distribution was observed by fluorescence
15 microscopy and fluorescence intensity was measured by fluorescence
16 spectrophotometer.

17 **RESULTS**

18 **Physiochemical properties of PLCL braided scaffold with/without PLL/HA** 19 **modification**

20 **Fourier-transform infrared spectroscopy of PLL/HA LBL modification**

1 The structure of PLCL fiber with/without PLL/HA modification are shown in Fig.1 by
2 FTIR. The spectra at 2990 cm^{-1} (PLLA), 2945 cm^{-1} (PLLA) and 2860 (PCL) cm^{-1}
3 demonstrated²⁹ the presence of alkyl group of copolymer PLCL. Bands at 1130 cm^{-1}
4 and 1065 cm^{-1} corresponded to ester backbone of PLA in scaffold SP and S1L
5 respectively.³⁰ The wavelength of PLL in SP was present as anion group³¹ at 1600 cm^{-1} .
6 The wavelength of HA in PLL/HA-PLL was present as carboxylate anion group³¹ at
7 1616 cm^{-1} and 1413 cm^{-1} . The wavelength of amine groups of PLL³¹ was shown at 1630
8 cm^{-1} in PLL/HA-PLL.

9 **Topology of PLL/HA LBL modification.**

10 PLL-FITC was observed to cover the fiber homogeneously by CLSM (Fig.2a), and
11 from SP to S1L the fluorescence intensity was increased. As shown in Fig.2b, the
12 surface of fiber was globally flat and smooth. Irregular polygonal structures on the
13 surface of SP were deduced to correspond to PLL molecules, while the “particles”
14 structures on S1L were attributed to HA molecules by AFM.

15 **Morphology of scaffold**

16 SEM images of PLCL braided scaffold in Fig.3a indicated a porous and braided
17 structure, and this multilayer structure was not influenced by PLL/HA modification.
18 For SB (scaffold without modification), the fibers kept the same texture from original
19 fabrication, while for SP and S1L the fibers presented a relatively smooth surface after
20 modification. The architecture of this multi-layer braided scaffold is illustrated in

1 Fig.3b: the scaffold was composed with six layers shown in six different colors (16
2 braided fibers each layer).

3 **Mechanical properties**

4 Typical stress-strain curves as well as Young's modulus evolution are exhibited in Fig.4.
5 Young's modulus of SB,SP and S1L were respectively 1616 ± 643 MPa, 1608 ± 156
6 MPa and 1758 ± 470 MPa. No significant changes in Young's modulus were therefore
7 observed. The three types of fibers broke for a strain around 15-25% with no significant
8 effect of surface modification.

9 **Biocompatibility of MSC-scaffold in vitro**

10 **MSC metabolic activity on scaffold**

11 Cell metabolic activity was detected by AB and is presented in Fig.5. The metabolic
12 activity of WJ-MSC on SB, SP and S1L increased of 24.2%, 19.64%, and 12.82%
13 respectively from day 1 to day 7. For BM-MSC, the activity increased of 21%, 15.77%
14 and 15.95% respectively on SB, SP and S1L from day 1 to day 7. Although cell
15 metabolic activities were improved both for WJ-MSC and BM-MSC from day 1 to
16 day 7, the cell metabolic activities decreased as the surface treatment went from SB to
17 SP and S1L, especially for WJ-MSC.

18 **MSC morphology and location on the scaffold**

19 The morphology of MSCs on the scaffold by SEM (Fig.6) showed that cells gathered to
20 form cell sheets between fibers, and also indicated ECM synthesis. Fluorescent images
21 (Fig.7) displayed a spindle and elongated shape of MSCs along the fibers. MSCs

1 tended to grow along the fiber direction in a homogeneous manner, migrated and
2 proliferated across fibers to form cell bridges. Quantification of morphological changes
3 of nucleus induced by scaffolds is illustrated in Fig.8. Mean nuclear area of WJ-MSC
4 ($224.7 \mu\text{m}^2$) was smaller ($p < 0.05$) than BM-MSC ($246.9 \mu\text{m}^2$) on tissue culture
5 polystyrene (TCPS). For WJ-MSC, the mean nuclear area did not change between
6 cells on scaffold and cells on TCPS. In contrast, for BM-MSC, the mean nuclear area
7 decreased for cells on SB and S1L compared to cell nucleus on TCPS. The nuclear
8 aspect ratio (length/width) of cells significantly increased ($p < 0.05$) comparing to cell
9 nucleus on TCPS for both WJ-MSC and BM-MSC.

10 **Extracellular matrix expression by MSC on the scaffold**

11 Results concerning collagen and tenascin-C expression are shown in Fig.9. Green
12 points on the scaffold correspond to collagen type I, collagen type III and tenascin-C
13 synthesized by WJ-MSC and BM-MSC respectively on day 14. It was observed that
14 both types of collagens and tenascin-C were substantially secreted, independently of
15 the surface modification.

16 **Chemotactic properties of scaffold on MSC**

17 Cell migration was performed to evaluate the effect of scaffold and scaffold
18 modification on MSCs chemotaxis. As observed on fluorescent images showed in
19 Fig.10, the number of migrated BM-MSC tended to be higher than WJ-MSC induced
20 by SB, SP and S1L, and this was confirmed by fluorescent intensity. It also
21 demonstrated that MSCs chemotaxis was most activated under the stimulation of S1L

1 for WJ-MSD and BM-MSD by fluorescent spectrophotometer.

2 **DISCUSSION**

3 PLCL³¹ is an elastomeric synthetic copolymer combining biocompatible, degradable
4 PLLA and PCL, resulting in desirable mechanical properties. It is of great interest in
5 tissue engineering,^{14,32} because of its biocompatibility, biodegradability, and
6 easy-processing. Vuornos et al³³ compared a foamed PLCL(70/30) structure with a
7 braided poly(L/D)lactide (PLA, 96L/4D) scaffold for tendon tissue engineering, and
8 PLCL was judged to be excessively elastic to form a braided structure in their study. On
9 the contrary, our group developed a controllable method to fabricate a uniform, porous,
10 braided structure based on elastic PLCL (85/15). Noteworthy, the number of fiber
11 layers could be adjusted to fulfill the mechanical requirements of different ligaments.
12 Moreover, PLL/HA layer-by-layer system was reported to be one of the classical PEM
13 for cell attachment, proliferation and ECM synthesis in many works.^{24, 25} In our study,
14 we introduced PLL/HA PEM on a braided PLCL scaffold for the first time and
15 confirmed by FTIR that PLL and HA were deposited on the surface of PLCL fibers^{29, 30,}
16 ³⁴. After the replacement of PLL by PLL-FITC, the fluorescence intensity was
17 increased from SP to S1L by CLSM. A polygonal and particle-like structure of PLL and
18 HA were additionally detected on scaffold by AFM.
19 The interaction between cells and biomaterials is influenced³⁵ by physicochemical
20 properties of scaffold (surface topography, surface toughness, wettability, stiffness, and
21 crystallinity), and also cell sources. PLL/HA modification could therefore influence the

1 scaffold surface microenvironment³⁶ as local mechanical, wettability, toughness and so
2 on. In a non-reported preliminary study, we firstly compared the deposition order of
3 PLL and HA by testing cell metabolic activity, and the results demonstrated that PLL
4 constitutes a cell-adhesive layer while HA is cell-repellent layer. PLL/HA
5 polyelectrolyte films have been previously reported³⁶ to be a pH-responsive PEM, and
6 both pH6.0-6.5 and pH7.4 have been applied for PLL/HA bilayer deposition prior to
7 the present study^{24, 36}. Based on these published data, the effects of pH (pH6.3 and
8 pH7.4) on PEM deposition was assessed and different PLL/HA bilayers numbers were
9 compared (reported in supplementary material) in order to optimize LBL modification
10 on scaffold for both WJ-MSC and BM-MSC. As a result, for both MSCs, cell
11 proliferation did not increase over one layer modification. Moreover, pH 6.3 for PEM
12 deposition greatly encouraged MSCs metabolic activity, especially for WJ-MSC
13 (reported in supplementary material). Consequently, in the present contribution, SB,
14 SP and S1L made in pH6.3 were selected.

15 Cell attachment, proliferation, ECM synthesis and migration are a series of
16 prerequisite activities for tissue regeneration. It is also modulated by bioactive
17 molecular such as growth factors. In the present study, MSCs attached well on
18 scaffolds as shown by the formation of cell sheets. There was no significant difference
19 of cell attachment between non-modified and modified scaffolds. Cell cytoskeleton
20 organization has been previously reported³⁷ to relate to cell fate on scaffold, to be
21 beneficial to predict cell commitment, and it also indicates cell senescence. Senescent

1 mesenchymal stem cells were characterized with enlarged, irregular morphology,
2 following with the decrease of phenotype and differentiation abilities³⁸. Fluorescent
3 images reported in the present study presented a spindle-shape cell cytoskeleton
4 covering the fibers. The nuclear size and shape were also related to the physiological
5 process³⁹ as cell senescence, differentiation, and diseases. The quantitative data of cell
6 nuclear morphology indicated an elongated and relatively spindle-like nuclear shape
7 with decreased nuclear area while increased aspect ratio for WJ-MS C and BM-MS C
8 on scaffold than on TCPS. Cells grew along the longitudinal direction of the fibers
9 which could be an adaptable, resistant cell-scaffold system to response to mechanical
10 stimulation. The results of Alamar Blue assay indicated that cell proliferated well on
11 scaffold, and the metabolic activity did not show significant change after PLL/HA
12 scaffold modification for WJ-MS C or for BM-MS C. Collagen constitutes the main
13 component of native ligament tissue⁴⁰, and its high expression is a basic requirement
14 for the formation of ligament-like extracellular matrix. In addition, Tenascin-C has
15 been shown to be a promising specific indicator⁴¹ of ligament ECM, and it has been
16 reported⁴² to be highly expressed in regenerative process of musculoskeletal tissue,
17 and to provide elasticity to tissues in reaction to heavy tensile loading. In the present
18 study, Collagen I, collagen III and tenascin-C were secreted by BM-MS C and
19 WJ-MS C on the scaffold within 14 days, which could have been encouraged by
20 ascorbic acid in the medium. This pointed out that BM-MS C-scaffold and
21 WJ-MS C-scaffold had potential in the future to form ligamentous tissue. Additionally,

1 other specific indicators as tenomodulin and scleraxis could have been characterized,
2 especially during a long-term culture including mechanical or biological stimulation.
3 Cell migration is a crucial step in the tissue healing process since cells firstly migrate
4 to the injury site or target area. Consequently, migration was assessed in present study
5 and our results showed that chemotaxis of WJ-MSC and BM-MSC was activated by
6 SB, SP and S1L. This migration was even more pronounced for one layer scaffold,
7 compared to SB and SP. This may show a possibility to recruit MSC for *in vivo*
8 implantation. These cell-scaffold constructs showed satisfying biocompatibility, and
9 the effect of growth factors incorporation into this PEM layer will be assessed in the
10 forthcoming developments.

11 **CONCLUSION**

12 A PLCL braided scaffold with PLL/HA modification was designed in our study. The
13 mechanical, morphological and biological results concerning the activity of WJ-MSC
14 and BM-MSC and the ECM synthesis showed that it may constitute a promising
15 scaffold for ligament tissue engineering. The incorporation of LBL increased cell
16 chemotaxis, which opens interesting perspectives for *in vivo* application. In the future,
17 the developed LBL technology will be used to incorporate growth factors on PLCL
18 braided scaffold in order to encourage tissue growth and the regeneration of a
19 functional ligamentous tissue.

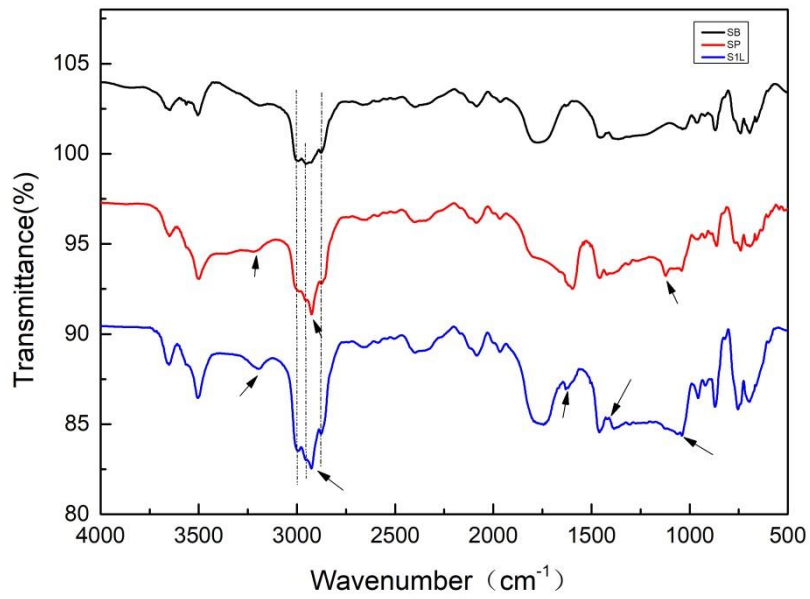
20 **REFERENCE**

21 1. Khan W. Ligament tissue engineering. Regen Strateg Treat Knee Jt Disabil.

- 1 Springer; 2017.
- 2 2. Barber JG, Handorf AM, Allee TJ, Li W-J. Braided nanofibrous scaffold for
3 tendon and ligament tissue engineering. *Tissue Eng Part A*. 2011;19:1265–1274.
- 4 3. Ge Z, Yang F, Goh JC, Ramakrishna S, Lee EH. Biomaterials and scaffolds for
5 ligament tissue engineering. *J Biomed Mater Res A*. 2006;77:639–652.
- 6 4. Leong NL, Petrigliano FA, McAllister DR. Current tissue engineering strategies
7 in anterior cruciate ligament reconstruction. *J Biomed Mater Res A*.
8 2014;102:1614–24.
- 9 5. Lavoie P, Fletcher J, Duval N. Patient satisfaction needs as related to knee stability
10 and objective findings after ACL reconstruction using the LARS artificial
11 ligament. *The Knee*. 2000;7:157–63.
- 12 6. Samuelsson K, Andersson D, Karlsson J. Treatment of Anterior Cruciate
13 Ligament Injuries With Special Reference to Graft Type and Surgical Technique:
14 An Assessment of Randomized Controlled Trials. *Arthrosc J Arthrosc Relat Surg*.
15 2009;25:1139–74.
- 16 7. Laurencin CT, Freeman JW. Ligament tissue engineering: An evolutionary
17 materials science approach. *Biomaterials*. 2005;26:7530–6.
- 18 8. Yagi M, Kuroda R, Nagamune K, Yoshiya S, Kurosaka M. Double-bundle ACL
19 reconstruction can improve rotational stability. *Clin Orthop*. 2007;454:100–107.
- 20 9. Kaeding CC, Aros B, Pedroza A, Pifel E, Amendola A, Andrish JT, Dunn WR,
21 Marx RG, McCarty EC, Parker RD. Allograft versus autograft anterior cruciate
22 ligament reconstruction: predictors of failure from a MOON prospective
23 longitudinal cohort. *Sports Health*. 2011;3:73–81.
- 24 10. Carlisle JC, Parker RD, Matava MJ. Technical considerations in revision anterior
25 cruciate ligament surgery. *J Knee Surg*. 2007;20:312–322.
- 26 11. Guarino V, Causa F, Ambrosio L. Bioactive scaffolds for bone and ligament tissue.
27 *Expert Rev Med Devices*. 2007;4:405–418.
- 28 12. Yang S, Leong K-F, Du Z, Chua C-K. The design of scaffolds for use in tissue
29 engineering. Part I. Traditional factors. *Tissue Eng*. 2001;7:679–689.
- 30 13. Cooper JA, Lu HH, Ko FK, Freeman JW, Laurencin CT. Fiber-based
31 tissue-engineered scaffold for ligament replacement: design considerations and in
32 vitro evaluation. *Biomaterials*. 2005;26:1523–32.
- 33 14. Laurent CP, Vaquette C, Martin C, Guedon E, Wu X, Delconte A, Dumas D,
34 Hupont S, Isla ND, Rahouadj R. Towards a tissue-engineered ligament: Design
35 and preliminary evaluation of a dedicated multi-chamber tension-torsion
36 bioreactor. *Processes*. 2014;2:167–179.
- 37 15. Laurent CP, Ganghoffer J-F, Babin J, Six J-L, Wang X, Rahouadj R.
38 Morphological characterization of a novel scaffold for anterior cruciate ligament
39 tissue engineering. *J Biomech Eng*. 2011;133:065001.
- 40 16. Lee J, Guarino V, Gloria A, Ambrosio L, Tae G, Kim YH, Jung Y, Kim S-H, Kim
41 SH. Regeneration of Achilles' tendon: the role of dynamic stimulation for

- 1 enhanced cell proliferation and mechanical properties. *J Biomater Sci Polym Ed.*
2 2010;21:1173–1190.
- 3 17. Ge Z, Goh JCH, Lee EH. Selection of cell source for ligament tissue engineering.
4 *Cell Transplant.* 2005;14:573–583.
- 5 18. Chen J, Altman GH, Karageorgiou V, Horan R, Collette A, Volloch V, Colabro T,
6 Kaplan DL. Human bone marrow stromal cell and ligament fibroblast responses
7 on RGD-modified silk fibers. *J Biomed Mater Res A.* 2003;67:559–570.
- 8 19. Cooper JA, Bailey LO, Carter JN, Castiglioni CE, Kofron MD, Ko FK, Laurencin
9 CT. Evaluation of the anterior cruciate ligament, medial collateral ligament,
10 achilles tendon and patellar tendon as cell sources for tissue-engineered ligament.
11 *Biomaterials.* 2006;27:2747–2754.
- 12 20. Van Eijk F, Saris D b. f., Riesle J, Willems W j., van Blitterswijk C a., Verbout A j.,
13 Dhert W j. a. Tissue Engineering of Ligaments: A Comparison of Bone Marrow
14 Stromal Cells, Anterior Cruciate Ligament, and Skin Fibroblasts as Cell Source.
15 *Tissue Eng.* 2004;10:893–903.
- 16 21. Tang Z, Wang Y, Podsiadlo P, Kotov NA. Biomedical applications of
17 layer-by-layer assembly: from biomimetics to tissue engineering. *Adv Mater.*
18 2006;18:3203–3224.
- 19 22. Costa RR, Mano JF. Polyelectrolyte multilayered assemblies in biomedical
20 technologies. *Chem Soc Rev.* 2014;43:3453–3479.
- 21 23. Sahoo S, Toh SL, Goh JC. A bFGF-releasing silk/PLGA-based biohybrid scaffold
22 for ligament/tendon tissue engineering using mesenchymal progenitor cells.
23 *Biomaterials.* 2010;31:2990–2998.
- 24 24. Yamanlar S, Sant S, Boudou T, Picart C, Khademhosseini A. Surface
25 functionalization of hyaluronic acid hydrogels by polyelectrolyte multilayer films.
26 *Biomaterials.* 2011;32:5590–5599.
- 27 25. Hahn SK, Hoffman AS. Characterization of biocompatible polyelectrolyte
28 complex multilayer of hyaluronic acid and poly-L-lysine. *Biotechnol Bioprocess*
29 *Eng.* 2004;9:179–183.
- 30 26. Pavesio A, Renier D, Cassinelli C, Morra M. Anti-adhesive surfaces through
31 hyaluronan coatings. *Med Device Technol.* 1997;8:20–1, 24–7.
- 32 27. Huang W-M, Gibson SJ, Facer P, Gu J, Polak JM. Improved section adhesion for
33 immunocytochemistry using high molecular weight polymers of L-lysine as a
34 slide coating. *Histochemistry.* 1983;77:275–279.
- 35 28. Zhang D, Zhang Y, Zheng L, Zhan Y, He L. Graphene oxide/poly-l-lysine
36 assembled layer for adhesion and electrochemical impedance detection of
37 leukemia K562 cancer cells. *Biosens Bioelectron.* 2013;42:112–118.
- 38 29. Kalpan G, Shalini VS, Jonnalagadda S, Kumar N. Fast degradable poly
39 (L-lactide-co-ε-caprolactone) microspheres for tissue engineering: synthesis,
40 characterization, and degradation behavior. *J Polym Sci A1.* 2007;45:2755–2764.
- 41 30. Xu J, Zhang J, Gao W, Liang H, Wang H, Li J. Preparation of chitosan/PLA blend

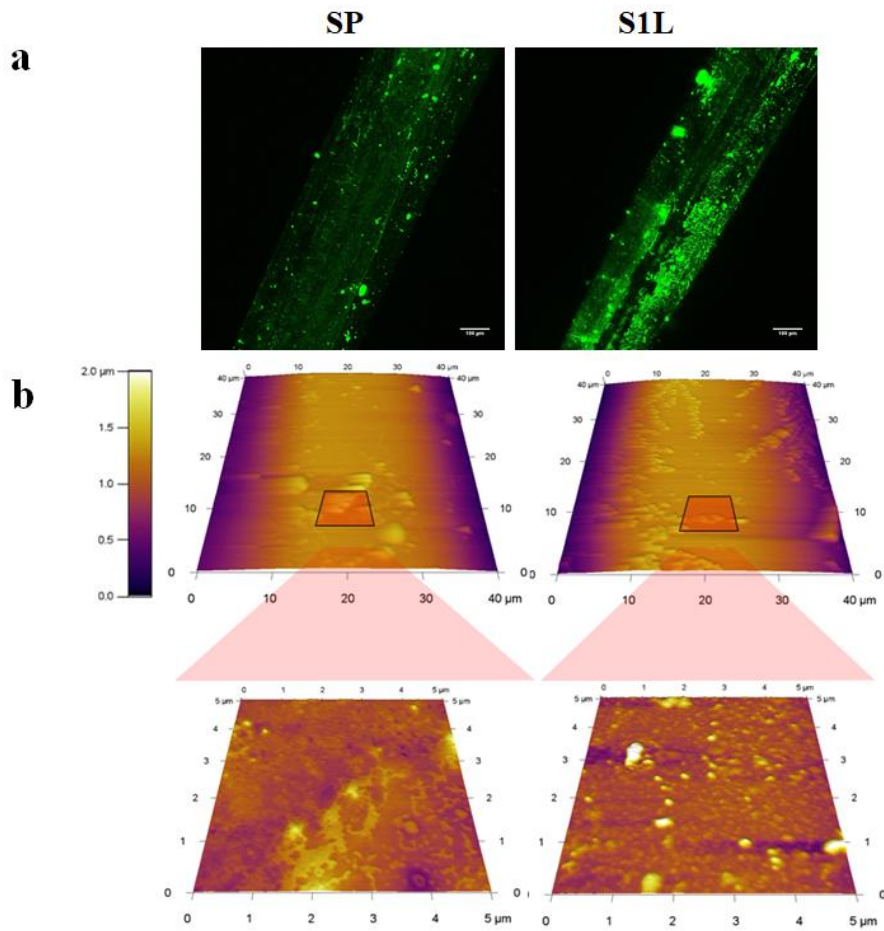
- 1 micro/nanofibers by electrospinning. *Mater Lett.* 2009;63:658–660.
- 2 31. Jeong SI, Kim B-S, Kang SW, Kwon JH, Lee YM, Kim SH, Kim YH. In vivo
3 biocompatibility and degradation behavior of elastic
4 poly(l-lactide-co- ϵ -caprolactone) scaffolds. *Biomaterials.* 2004;25:5939–46.
- 5 32. Vaquette C, Kahn C, Frochot C, Nouvel C, Six J-L, De Isla N, Luo L-H,
6 Cooper-White J, Rahouadj R, Wang X. Aligned poly(L-lactic-co- ϵ -caprolactone)
7 electrospun microfibers and knitted structure: A novel composite scaffold for
8 ligament tissue engineering. *J Biomed Mater Res A.* 2010;94A:1270–82.
- 9 33. Vuornos K, Björninen M, Talvitie E, Paakinaho K, Kellomäki M, Huhtala H,
10 Miettinen S, Seppänen-Kaijansinkko R, Haimi S. Human adipose stem cells
11 differentiated on braided polylactide scaffolds is a potential approach for tendon
12 tissue engineering. *Tissue Eng Part A.* 2016;22:513–523.
- 13 34. Amorim S, Martins A, Neves NM, Reis RL, Pires RA. Hyaluronic
14 acid/poly-L-lysine bilayered silica nanoparticles enhance the osteogenic
15 differentiation of human mesenchymal stem cells. *J Mater Chem B.* 2014;2:6939–
16 6946.
- 17 35. Lutolf MP, Hubbell JA. Synthetic biomaterials as instructive extracellular
18 microenvironments for morphogenesis in tissue engineering. *Nat Biotechnol.*
19 2005;23.
- 20 36. Burke SE, Barrett CJ. pH-Responsive Properties of Multilayered
21 Poly(l-lysine)/Hyaluronic Acid Surfaces. *Biomacromolecules.* 2003;4:1773–83.
- 22 37. Treiser MD, Yang EH, Gordonov S, Cohen DM, Androulakis IP, Kohn J, Chen CS,
23 Moghe PV. Cytoskeleton-based forecasting of stem cell lineage fates. *Proc Natl*
24 *Acad Sci.* 2010;107:610–615.
- 25 38. Wagner W, Horn P, Castoldi M, Diehlmann A, Bork S, Saffrich R, Benes V, Blake
26 J, Pfister S, Eckstein V, Ho AD. Replicative Senescence of Mesenchymal Stem
27 Cells: A Continuous and Organized Process. *PLOS ONE.* 2008;3:e2213.
- 28 39. Chen B, Co C, Ho C-C. Cell shape dependent regulation of nuclear morphology.
29 *Biomaterials.* 2015;67:129–36.
- 30 40. Altman G, Horan R, Martin I, Farhadi J, Stark P, Volloch V, Vunjak-Novakovic G,
31 Richmond J, Kaplan DL. Cell differentiation by mechanical stress. *FASEB J.*
32 2002;16:270–2.
- 33 41. Altman GH, Horan RL, Lu HH, Moreau J, Martin I, Richmond JC, Kaplan DL.
34 Silk matrix for tissue engineered anterior cruciate ligaments. *Biomaterials.*
35 2002;23:4131–41.
- 36 42. Jarvinen TAH. Mechanical loading regulates the expression of tenascin-C in the
37 myotendinous junction and tendon but does not induce de novo synthesis in the
38 skeletal muscle. *J Cell Sci.* 2003;116:857–66.
- 39
40



1

2 Fig1. FTIR of PLL/HA modified on PLCL scaffold (SB:PLCL scaffold blank, SP:
3 PLCL-PLL, S1L: PLCL-PLL/HA-PLL).

4

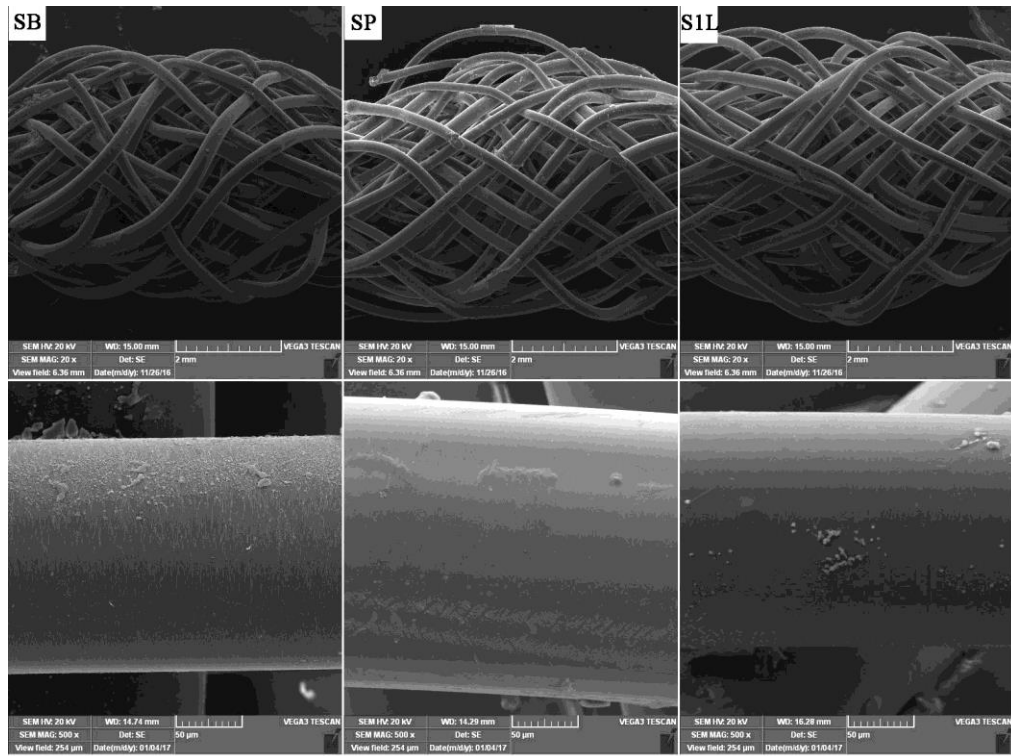


1

2 Fig2. Morphology of PLL-FITC/HA on PLCL fiber by CLSM (a), and topology of
 3 PLL/HA on PLCL fiber by AFM (b).(SP: PLCL scaffold-PLL-FITC, S1L: PLCL
 4 scaffold-PLL/HA-PLL).

5

6



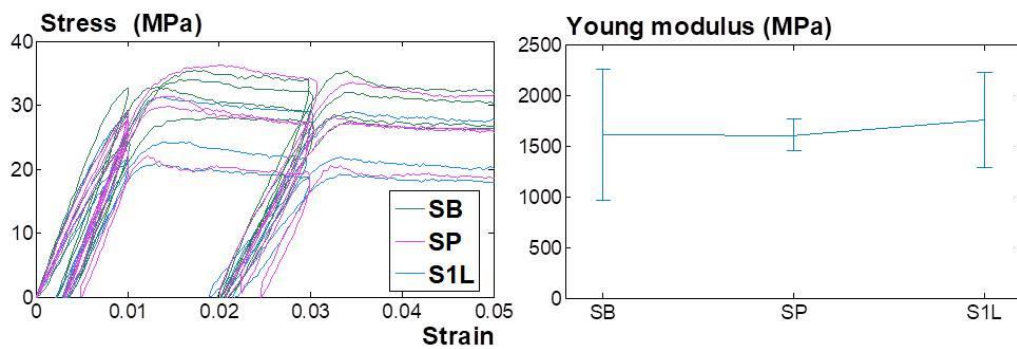
1

2 Fig3. Morphology of PLCL scaffold and PLCL scaffold modified with PLL/HA by

3 SEM. (SB:PLCL scaffold blank, SP: PLCL-PLL, S1L: PLCL-PLL/HA-PLL).

4

5



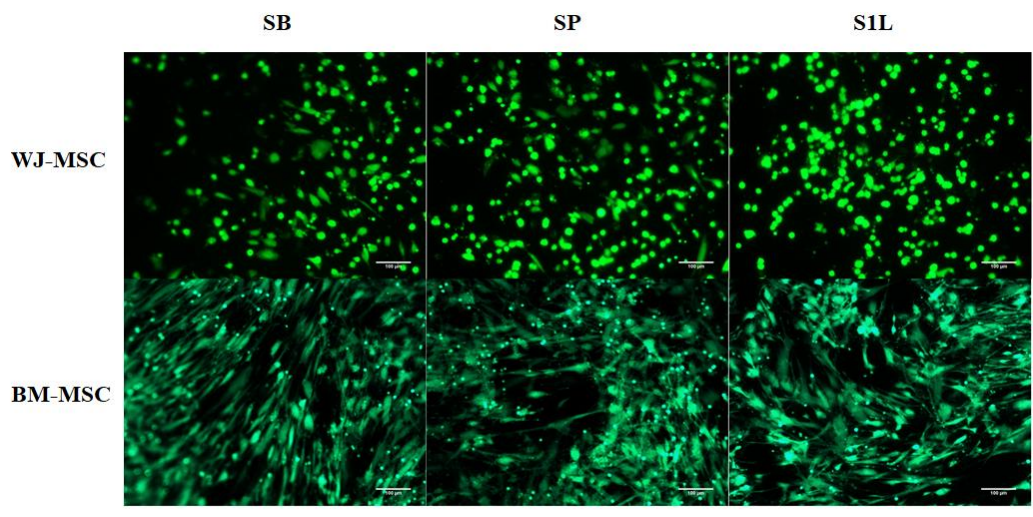
6

7 Fig4. Mechanical test of PLCL fibers (SB:PLCL fiber blank, SP: PLCL fiber-PLL, S1L:

8 PLCL fiber-PLL/HA-PLL).

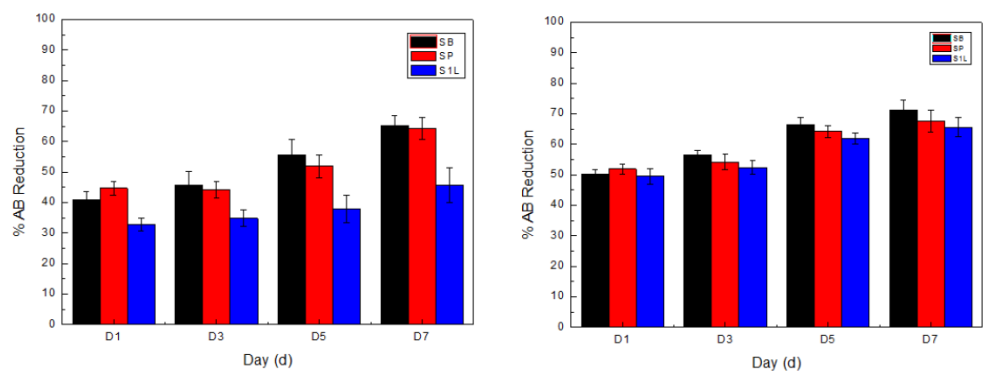
9

1
2
3
4
5
6
7
8



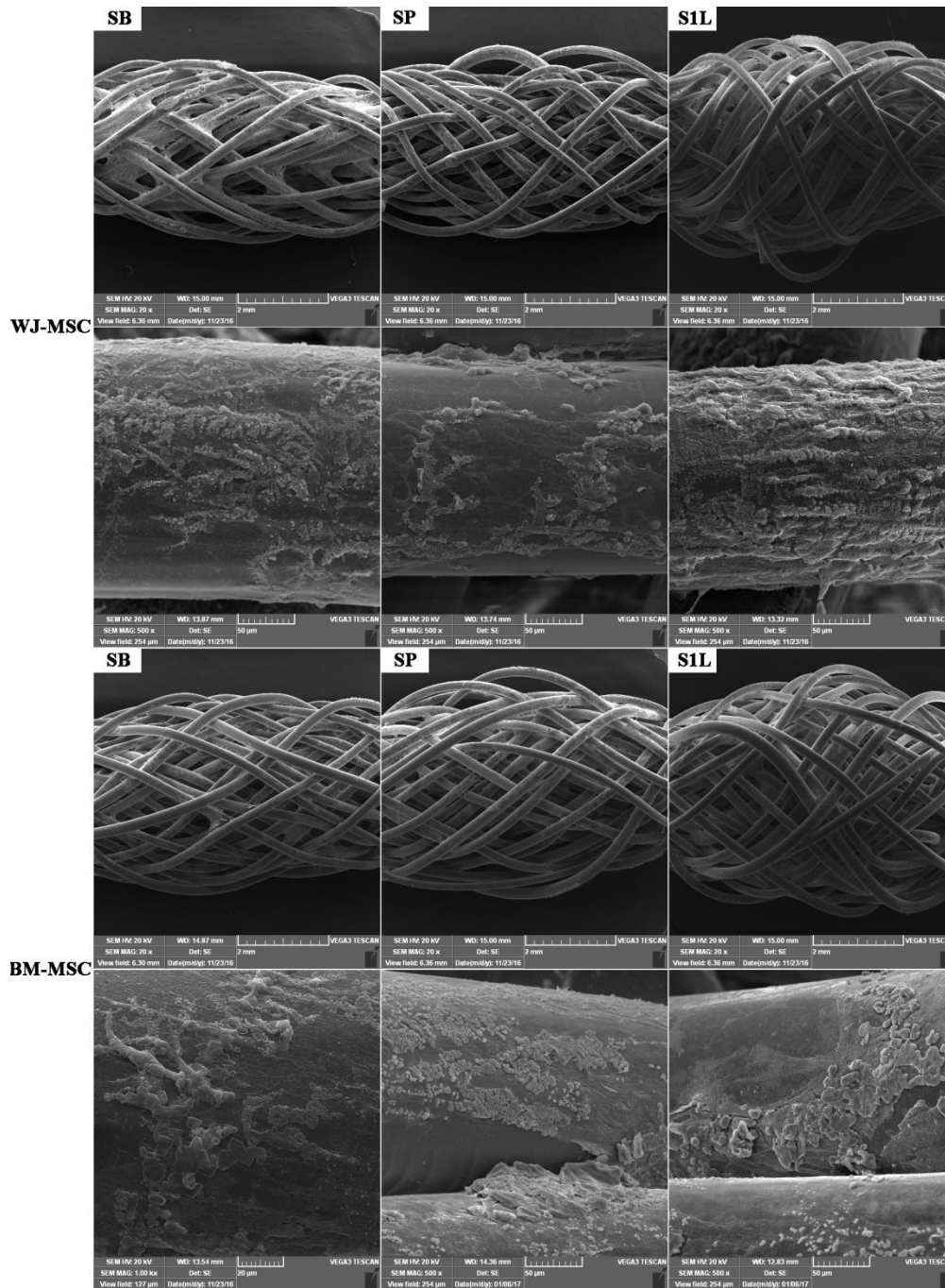
9
10

11 Fig5. Migration of WJ-MSC and BM-MSC induced by PLCL scaffold, scaffold-PLL
12 and scaffold- PLL/HA-PLL.



1

- 2 Fig6. Reduction of AB of WJ-MSC and BM-MSC on PLCL scaffold (SB:PLCL
 3 scaffold blank, SP: PLCL-PLL, S1L: PLCL-PLL/HA-PLL).



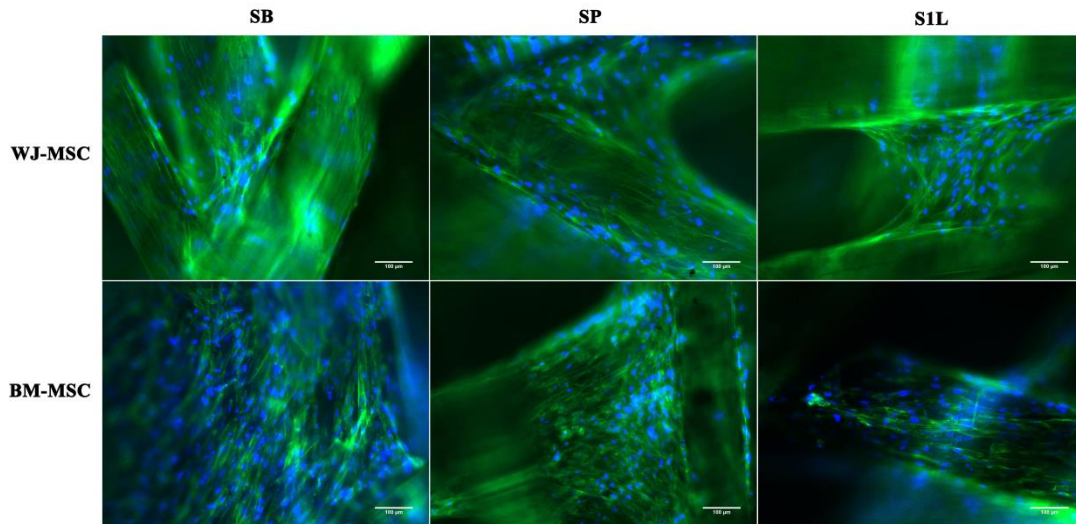
1

2 Fig7. Morphology and distribution of WJ-MSC and BM-MSC on scaffold by SEM.

3 (SB:PLCL scaffold blank, SP: PLCL-PLL, S1L: PLCL-PLL/HA-PLL).

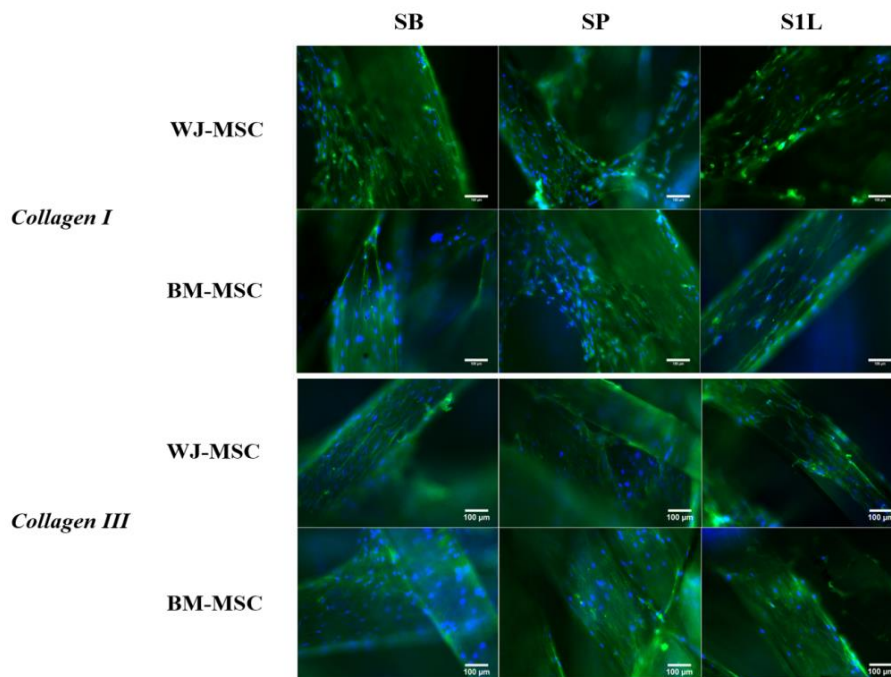
4

5



1

2 Fig8. Morphology and distribution of WJ-MSC and BM-MSC on scaffold by
 3 florescence microscopy.(SB: PLCL scaffold blank, SP: PLCL-PLL, S1L:
 4 PLCL-PLL/HA-PLL).



5

6 Fig9. Collagen I and collagen III expression by WJ-MSC and BM-MSC on PLCL
 7 scaffolds on D14. (SB:PLCL scaffold blank, SP: PLCL-PLL, S1L:
 8 PLCL-PLL/HA-PLL).